Available online at www.sciencedirect.com

ScienceDirect

Procedia CIRP 125 (2024) 243–248

www.elsevier.com/locate/procedia

CIRP BioM 2024

Ultrathin Polymeric Platform for Drug-Eluting Stent: A proof of concept

Bosch, A.[a,b], Casanova-Batlle, E.[b], Ausellé-Bosch, S.[c], Polonio-Alcalá, E.[c], Puig, T.[c], Ciurana, J.[b] and Guerra, A.J.[a,*]

[a]*Eurecat, Technology Centre of Catalonia, Unit of Advanced Manufacturing Systems, 08290 Cerdanyola del Vallès, Spain*
[b]*Product, Process and Production Engineering Research Group (GREP), Department of Mechanical Engineering and Industrial Construction, University of Girona, 17003 Girona, Spain*
[c]*New Therapeutic Targets Laboratory (TargetsLab) – Oncology Unit, Department of Medical Sciences, Faculty of Medicine, University of Girona, 17003 Girona, Spain*

* Corresponding author. Tel.: +34 678-384-821. *E-mail address:* antonio.guerra@eurecat.org

Abstract

Recent innovations in Drug-Eluting Stents (DES) technology have led to the development of new stents with further reduction in strut width, the ultrathin DES, with struts thinner than 70 µm. Ultrathin DES may further improve the efficacy and safety profile of Percutaneous Coronary Intervention (PCI) by reducing the risk of target-lesion and target-vessel failures compared to the current-generation DES. However, the ultrathin DES metallic platform still presents some associated problems, such as biofilm formation, infection, and migration, all related to the cellular response.

The present work aims to produce an ultrathin permanent polymeric platform for a new generation of polymeric drug-eluting stents (PDES). In this work, the cellular response was compared with the traditional stainless steel (SS316L) and polycaprolactone (PCL) to determine whether these polymers could address this challenge. An innovative method of tubular 3D micro stereolithography tubular (ST3DT) was used. Different PDES platforms were fabricated with different polymeric materials (based on polyurethane and urethane dimethacrylate). Subsequently, HFL1 fibroblasts were seeded on the PDES, PCL and SS316L for 3 days. The findings from the assays of cell biocompatibility and proliferation (75%PCL), coupled with the successful fabrication of stent struts below 70 µm using the Surgical Guide resin and the ST3DT method, suggest that resin is a promising candidate for a PDES.

Keywords: stent; medical devices; additive manufacturing; stereolithography.

1. Introduction

One of the leading causes of morbidity and mortality worldwide is coronary artery disease a condition characterized by the narrowing of the artery due to plaque deposits [1]. Due to its effectiveness, drug-eluting stents (DES) are vascular tubular prostheses widely used for the treatment of blood ducts partially or totally closed by arteriosclerosis. DES were developed in 2002 to reduce neointimal hyperplasia (NIH) caused by their predecessors, known as Bare Metal Stents (BMS), after a Percutaneous Coronary Intervention (PCI). First-generation DES were based on a stainless-steel platform coated with a drug-eluting durable polymer but had an increased incidence of very late thrombosis [2], caused by an incomplete endothelization and hypersensitivity to the polymer coating with inflammation of the endothelium.

Second-generation DES were developed in 2008 to overcome the clinical limitations reported by studies and trials. This generation was focused on improving the strut width, deliverability, and flexibility [1]. Also, biocompatible and biodegradable polymers coatings were introduced in this generation, leading to a revolutionary transformation [3]. To tackle all the drawbacks that are still present in DES technology, a new generation of ultrathin stents [4] has begun

10.1016/j.procir.2024.08.042

to be studied. The thinner struts permit the stent to be more flexible, improving its trackability and crossability, and to be less prone to stent thrombosis (ST) [5]. Moreover, ultrathin stent presents better deliverability [6], which reduces the trauma caused in the vessel wall, leading to a minimal inflammatory response and rapid endothelialization. Clinical trials with ultrathin DES have demonstrated promising outcomes [6]. The next generation DES have to improve endothelialization and rapid arterial healing [7]. Since hemodynamics is crucial in endothelialization, reducing the struts is a crucial aspect of the development of better stents. The strut width reduction implies a decrease in hemodynamics perturbations, fostering the migration of endothelial cells (EC) to the site of implantation [8], leading to faster endothelialisation and preventing restenosis. Numerous investigations have delved into improving the polymeric coating of DES, yet the incorporation of a permanent polymeric core remains largely unexplored. Furthermore, there are no commercially available stents manufactured with vat polymerization technology, therefore, the potential of the technology is not being exploited to overcome the limitations of the technologies studied. This work endeavors to address the imperative need for advancements in polymeric ultrathin stent fabrication through the integration of a novel technology. Firstly, the work aims to study the cell viability of different commercial non-biodegradable resins and to study cell proliferation in solid tubular scaffolds, comparing the outcomes with widely studied materials such as PCL and SS316L. Secondly, the paper aims to demonstrate the feasibility of manufacturing polymeric ultrathin stents.

Nomenclature

BMS	Bare Metal Stent
C	Clear
DES	Drug-Eluting Stents
EC	Endothelial cells
IPA	Isopropyl alcohol
L	Length
NCS	Newborn Calf Serum
NHI	Neointimal Hyperplasia
PBS	Phosphate Buffered Solution
PCI	Percutaneous Coronary Intervention
PCL	Polycaprolactone
PDES	Polymeric Drug-Eluting Stents
R	Rigid
SG	Surgical Guide
SS316L	Stainless Steel 316L
ST	Stent Thrombosis
ST3DT	STereolithography 3D Tubular
S_T	Stent Thickness
S_w	Strut Width
T	Tough

2. Materials and Methods

2.1. Materials

Four different resins were compared with PCL and SS316L. The resins were methacrylate-based resin (Clear (C), FLGPCL04). and urethane dimethacrylate-based resin (Tough (T), FLTO1501), (Rigid 4000 (R), FLRGWH01), and (Surgical Guide (SG), FLSGAM01). The resins were supplied by Formlabs (Formlabs, OH, US).

96º Isopropyl alcohol (IPA) (Quimimont, Barcelona, Spain) was used to clean the non-photopolymerized resin present in the fabricated stent before curing.

PCL CAPA 6500 (Perstorp, Mälmo, Sweden) was used for its biocompatibility.

SS316L tubes were supplied by tuboscapilares based in Spain. SS316L has been used because it is widely used in commercial stents and many medical devices due to its high biocompatibility, radio-opacity, and corrosion resistance.

2.2. Ultra-thin stent fabrication

2.2.1. ST3DT

ST3DT is a method based on vat polymerization technology. The novel system is based on the introduction of a tubular bed. The machine was presented by Bosch et al. [9]. The ST3DT is equipped with a 500 mW and 405 nm wavelength gaussian laser attached to a fiber optic collimator (ThorLabs, New Jersey, US). The main advantages of this method are the capability to fabricate tubular prostheses without support material, eliminating the lamination of the object from the cartesian approach, allowing the fabrication of a stent in less than 1 minute, drastically reducing the amount of material used and waste, and allowing multi-material fabrication and 3D-relief over the stents' surface. Stents and tubes were fabricated with the parameters (Table 1) found in a screening experiment of previous works [9].

Table 1. Parameters used for the stent and tube fabrication for each resin.

Resin	Exposure [mJ/mm^2]	Curing Time (min)	Curing Temperature (ºC)
Surgical Guide	3	30	70
Clear	5	30	60
Tough	7	60	60

FormLabs Washing Station and FormLabs Cure Station (FormLabs, Massachusetts, USA) were used to wash and cure the stents and tubes. After the print, the samples were washed for 5 minutes in IPA and dried prior to curing. The equipment allows samples to be cured with 13 multi-directional LED, with a total power of 39 W at 405 nm wavelength.

2.2.2. Dip coating

PCL tubes were fabricated by dip coating from a 15% w/v solution in acetone (Amidata RS, Spain) on SS316L tubes, taking advantage of a 3D Printer (Prusa MKS3, Prusa

Research, Czech Republic) following the method described by Guerra et al. [10]. PCL tubes were fabricated with an introduction and withdrawal speed of 200 mm/min for 5 cycles and 60 seconds of drying time between cycles.

2.2.3. Stent model

The stent model used for experiments was a Palmaz-Schatz. geometry cell characterized by the following parameters: 6 mm of inner diameter ($I_{\emptyset}$), 20 mm of length (L), 6 circumferential cells ($N_{C,y}$), 6 longitudinal cells ($N_{C,x}$), and 70µm strut width (S_w) (Fig. 1. (a) CAD of the stent fabricated (b) 3D detail of a single diamond-shaped cell and a cross-section of the stent with key parameters

.a). Its geometric simplicity makes it a perfect candidate to study the parameter that defines ultrathin stents, the strut width (Fig. 1.b). The stent was designed to be 6 mm in inner diameter ($I_{\emptyset}$) and 20 mm in length (L). Strut width (S_w) is a key factor in the hemodynamics within the blood vessel. Hemodynamics is critical to endothelialization after cardiovascular stent implantation [11].

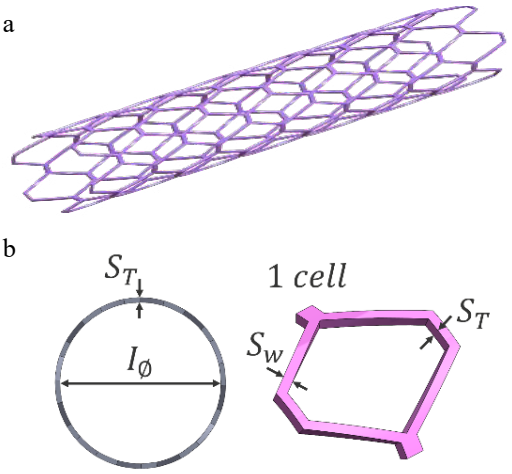

Fig. 1. (a) CAD of the stent fabricated (b) 3D detail of a single diamond-shaped cell and a cross-section of the stent with key parameters

For the study of cytotoxicity, flat probes with a total surface area of 125 mm^2 were fabricated to submerge in the culture medium for 24 h. For the study of cell adhesion, solid tubes were used to maximize the surface area but at the same time to study the most unfavorable case, because tubes did not contain pores, but simply a surface with a specified roughness. The tubes were 6 mm in diameter and 10 mm in length, thickness of the tubes differed due to the different fabricating processes, ranging from 0.1 mm for resin tubes (ST3DT), 0.2 mm for PCL tubes (dip coating), and 0.5 mm for SS316L tubes (extrusion).

2.3. Stent cell culture

2.3.1. Cell Line

Human HFL1 fibroblasts were purchased from the American Type Culture Collection (ATCC, Rockville, MD, USA). Cells were cultured in Kaighn's Modification of Ham's F-12 (F-12K; Corning Inc. Life Sciences, Tewksbury, MA, USA) supplemented with 10% fetal bovine serum (FBS) (HyClone, Logan, UT, USA) and 50 U/mL penicillin/streptomycin (Lonza, Walkersville, MD, USA). Cells were maintained in a 5% CO_2 humidified incubator at 37ºC. Cells were tested for mycoplasma contamination regularly.

2.3.2. Scaffold Sterilization

After the planar samples and the tubes were cured, they were sterilizated with an autoclave at 121 ºC, 90% humidity and 2 atm for 15 minutes. Then they were dried at room temperature for 30 minutes. SS316L samples also were sterilized in the autoclave. PCL tubes were sterilizated with 70% v/v ethanol/water solution overnight, washed twice with Phosphate Buffered Solution (PBS) (Sigma Aldrich, Saint Louis, USA) and exposed to UV light for 30 minutes as Rabionet et al. done for tubular and non-tubular scaffolds [12].

2.3.3. Cell Culture

For biocompatibility assay, sterilized planar samples were submerged into 3 ml of medium F-12K (ATCC, VA, US) for 72 h at 37ºC and 5% CO_2. Then, the samples were removed, and cells were exposed to the resulting medium for 24h at 37ºC and 5% CO_2. Afterwards, following the ISO 10993, cell viability was analyzed using MTT assay.

For the cell adhesion and the cell proliferation experiments, sterilized materials were placed in 24-well non-adherent microplates (Starstedt, Nümbrecht, Germany) and soaked in Newborn Calf Serum (NCS) (ATCC, VA, US) for 2 hours at 37ºC. After removing the serum, 250.000 HFL1 cells were seeded by immersion, and the tubes were incubated for 24 and 72 hours at 37ºC and 5% CO_2, as described by previous studies from our group [13], [14].

MTT (3-4.5-dimethyl-2-thiazolyl)-2.5-diphenyltetrazolium bromide) assay was selected to test fibroblast viability on tubular scaffolds. MTT is a tetrazolium-based colorimetric assay widely adopted for biocompatible evaluation. The MTT is reduced by the viable cells and produce purple crystals of formazan, which can be solubilized by dimethyl sulfoxide (DMSO) into a colored solution. Hence, the absorbance of the DMSO solution is related to the cell number.

2.4. Characterization

The S_W of the stents was measured with the Optical Microscopy with Microscope Nikon SMZ-745T attached to a digital camera CT3 ProgRes. ImageJ was used to process the images and collect the data for evaluation.

The rugosity of the fabricated tubular samples was examined using Roughness Mitutoyo SurfTest SV-2000. R_a and R_q were measured for each material. The machine was equipped with 2 μm radius tip and λ_c was set to 2.5 and λ_s at 0.008.

3. Results and Discussion

This section presents the results of the manufacturing process and the surface analysis, focusing on the outputs achieved for each type of resin. Cell viability, adhesion, and proliferation results are also showed.

3.1. Biocompatibility Assay

The results indicated the cell viability of the resins (Fig. 2.), except for the rigid resin, which is below 75%, the limit established to be considered biocompatible. In this first validation, resins C and SG showed better results than PCL and SS316L. However, these results were not conclusive. Although T resin showed lower cell viability than C and SG, it meets the requirement and is not discarded as R. The results obtained with PCL and SS316L were consistent with previous research, validating the results obtained.

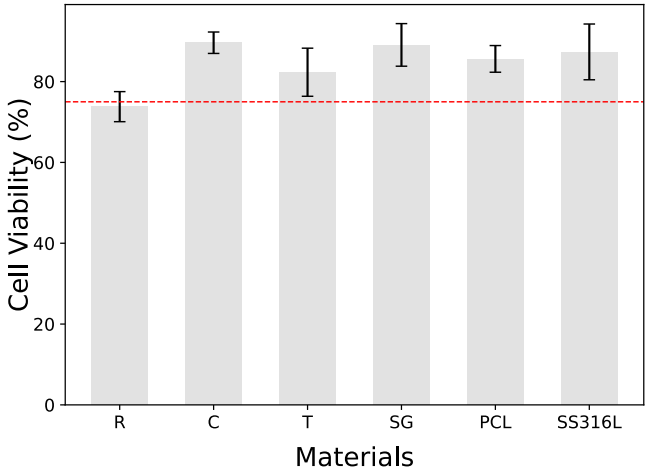

Fig. 2. Bar plot depicting cell viability (%) from the control (cells not exposed to any material) (n=3). Values below 75% (red line) should not be considered due to its lack of biocompatibility

3.2. Cell Adhesion

The results of cell adhesion at 24h pointed out that the cells adhere sufficiently to the scaffolds fabricated by vat polymerization, but with slight variability.

Steel was the material with the highest cell adhesion rate, even higher than that of PCL, the reference material. However, the cells attached to the SS316L made a sort of aggregates or films. Therefore, it may be that the cell adhesion on the steel is lower than what we were observing with the MTT assay.

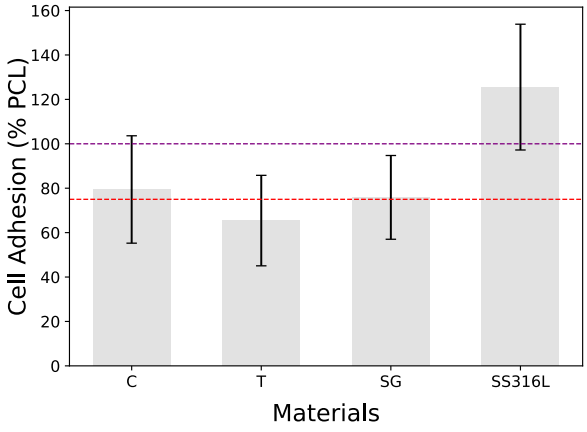

Fig. 3. Bar plot depicting cell adhesion (%) for each material compared to reference (PCL, purple line) (n=3). Values below 75% (red line) should not be considered due to its lack of biocompatibility.

Although the results evidenced that after 24h the cell adhesion in the resin tubes was lower than the reference material, the experiment verified that HFL-1 cells adhere to the surface of the different materials (Fig. 3.). Consequently, proliferation experiments could be performed.

3.3. Cell Proliferation

After 72 hours of incubation, it can be observed in Fig. 4. that all materials exhibited higher cell proliferation than PCL, the reference material.

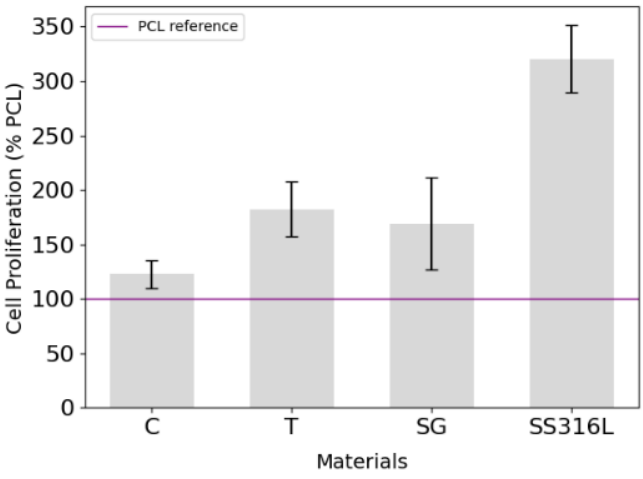

Fig. 4. Bar plot depicting cell proliferation (%) compared to reference material (PCL after 72h, purple line), comparative cellular response across the studied materials (n=3).

However, cell proliferation occurred on both the outer and inner surfaces only in the PCL tubes. SS316L presented the highest cell proliferation rate, almost duplicating the initial number within 3 days. As can be seen in Fig. 5. all resins showed good adhesion and cell proliferation. The purple colour

intensity is related to the concentration of living fibroblasts cells present on the scaffold surface.

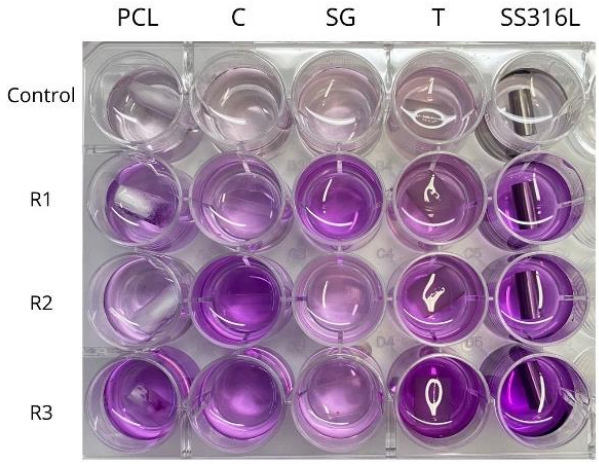

Fig. 5. Cell proliferation results after MTT assay. First row is for negative control. Purple spots represent formazan crystals and, therefore, fibroblast localization after 3 culture days on tubular scaffolds.

3.4. Manufacturing Process: Ultrathin stents

Manufacturing process has shown a great stability being able to manufacture replicas with almost 100% of likeness. As can be seen in Fig. 6., SG resin exhibited the thinnest strut width (M=68.653 µm, SD=0.85). Similar values were achieved for C resin (M=70.865 µm, SD=0.748), but slightly above the ultrathin limit. On the other hand, achieving thin struts and maintaining process stability proved unattainable with the T resin (M=193.43 µm, SD=24.178), leading to exclude it. The main reasons may include its low critical exposure point (where it starts to polymerize), which falls significantly below the minimum power threshold of the installed laser. Nevertheless, mechanical properties of T resin are interesting and should be considered in a future.

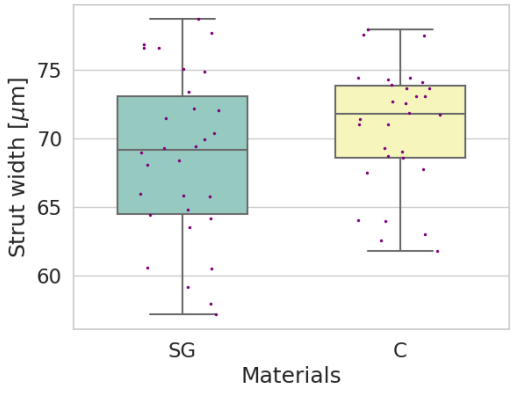

Fig. 6. Box plot for strut width achieved for SG and C resins, with the parameters described previously. Purple points represents the measures for the 3 replicas.

From earlier research, it was affirmed that laser power and printing feedrate play a crucial role in the process. To reach thinner struts, decreasing the laser power while increasing the feedrate is the most effective strategy. Furthermore, the optimal impregnation layer over the shaft was achieved by partially submerging it in the vat. The promising results open a wide range of possibilities while offering considerable benefits to stenting research field. The technology used in this work has demonstrated its potential to create small tubular prostheses with ultrathin struts (Fig. 7.).

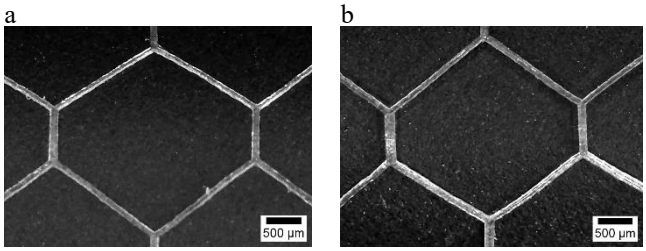

Fig. 7. Optical microscope images for random cells (a) Surgical Guide resin replica 3; (b) Clear resin replica 3.

3.5. Rugosity

The calculated roughness of each material showed the differences in surface finish depending on the material used and on the manufacturing technology. Within the tubular scaffolds manufactured by vat polymerization, the differences were substantial especially between SG (M=1.570 µm, SD=0.11) and C (M=10.690 µm, SD=0.84), where the calculated Ra was approximately 7 times higher in C. Results for T (M=3.503 µm, SD=0.11) fell between the two previous. Tubes fabricated with non-photopolymerizable material showed a lower rugosity, PCL (M=1.078 µm, SD=0.28) and SS316L (M=0.630 µm, SD=0.05). However, in all resins the results were in the microscale. Results showed a trend between roughness and cell adhesion, since the lower the Ra, the higher the cell adhesion (Fig. 8.). A trend is also seen in cell proliferation, where roughness closer to the nanoscale promotes higher cell proliferation, consistent to literature [15]. The results indicated that surfaces' roughness close to the nano-scale are desirable to foster cell adhesion and proliferation [16], and a surface post-treatment should be performed to reach the optimal roughness for the resins.

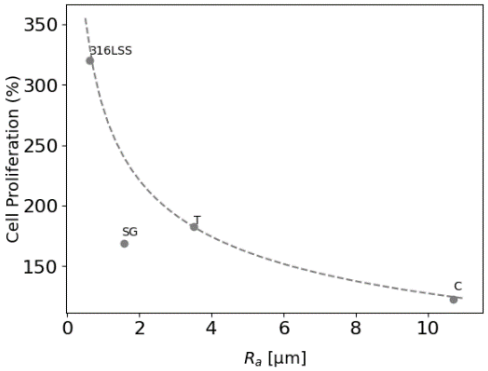

Fig. 8. Plot depicting the relation of the cell proliferation with rugosity for each material.

4. Conclusions

The findings from the assays of cell viability and proliferation, coupled with the successful fabrication of stent struts below 70 µm using the Surgical Guide resin and the ST3DT method, suggest that this resin holds promise as a suitable candidate for the foundation of a PDES. Nevertheless, it is imperative to emphasize that mechanical testing remains a crucial step in studying the feasibility, as the stent must meet to severe mechanical requirements.

It is worth pointing out that the ST3DT technology is not optimal for the manufacture of solid tubes, as the stents do not have any kind of lamination, the roughness will be lower than the one obtained.

Furthermore, the necessity to develop alternative resins with enhanced safety and efficacy, minimizing residues that could potentially enter the cardiovascular system, is evident. Addressing these concerns calls for focused efforts in surface engineering to attain a more biocompatible stent.

The biocompatibility challenges experienced with certain commercial resins highlights the importance of proper printing and postprocessing techniques, and the evaluation methods after printing. In the contemporary discourse surrounding polymeric resins for medical devices, safety concerns take center stage, underscoring the critical need to reduce the quantity of non-reacted monomers [17].

As we persist in the quest for the ideal stent, future research endeavors should prioritize the development of novel materials that can serve diverse functions, including serving as a base material, coating, or drug carrier, thereby contributing to the continual advancement of stent technology.

5. Acknowledgements

This work was financially supported by the Catalan Government through the funding grant ACCIÓ-Eurecat (Project TRAÇA2023-DESTOFU). A. Bosch is a fellow of Eurecat's "Vicente López" PhD grant program. This work was funded by PLEC2021-007523 / AEI / 10.13039/501100011033 and by the European Union – NextGenerationEU. It was also supported by Spanish grant from Instituto de Salud Carlos III and co-funded by European Union ERDF/ESF, "A way to make Europe"/"Investing in your future") (PI19/00372). The authors thank the support of Catalan Government (2021SGR01589). The authors thank Research Technical Services from the University of Girona.

6. References

[1] Scafa Udriște A, Niculescu A-G, Grumezescu AM, Bădilă E. Cardiovascular Stents: A Review of Past, Current, and Emerging Devices. Materials 2021; 14, 2498.

[2] Daemen J, Wenaweser P, Tsuchida K, Abrecht L, Vaina S, Morger C, Kukreja N, Jüni P, Sianos G, Hellige G, Van Domburg RT, Hess OM, Boersma E, Meier B, Windecker S, Serruys PW. Early and late coronary stent thrombosis of sirolimus-eluting and paclitaxel-eluting stents in routine clinical practice: data from a large two-institutional cohort study. The Lancet 2007; 369, 667-678.

[3] Borhani S, Hassanajili S, Ahmadi Tafti SH, Rabbani S. Cardiovascular stents: overview, evolution, and next generation. Prog Biomater 2018; 7, 175-205.

[4] Buiten RA, Zocca P, Von Birgelen C. Thin, very thin, or ultrathin-strut biodegradable or durable polymer-coated drug-eluting stents. Current Opinion in Cardiology 2020; 35, 705-711.

[5] Bangalore S, Toklu B, Patel N, Feit F, Stone GW. Newer-Generation Ultrathin Strut Drug-Eluting Stents Versus Older Second-Generation Thicker Strut Drug-Eluting Stents for Coronary Artery Disease: Meta-Analysis of Randomized Trials. Circulation 2018; 138, 2216-2226.

[6] Gherasie F-A, Valentin C, Busnatu S-S. Is There an Advantage of Ultrathin-Strut Drug-Eluting Stents over Second- and Third-Generation Drug-Eluting Stents? JPM 2023; 13, 753.

[7] Khan W, Farah S, Domb AJ. Drug eluting stents: Developments and current status. Journal of Controlled Release 2012; 161, 703-712.

[8] Marei I, Ahmetaj-Shala B, Triggle CR. Biofunctionalization of cardiovascular stents to induce endothelialization: Implications for in- stent thrombosis in diabetes. Front. Pharmacol. 2022; 13, 982185.

[9] Bosch A, Casanova-Batlle E, Constantin I, Rubio C, Ciurana J, Guerra AJ. An Innovative Stereolithography 3D Tubular Method for Ultrathin Polymeric Stent Manufacture: The Effect of Process Parameters. Polymers 2023; 15, 4298.

[10] Guerra AJ, San J, Ciurana J. Fabrication of PCL/PLA Composite Tube for Stent Manufacturing. Procedia CIRP 2017; 65, 231-235.

[11] Nguyen DT, Smith AF, Jiménez JM. Stent strut streamlining and thickness reduction promote endothelialization. J. R. Soc. Interface. 2021; 18, 20210023.

[12] Rabionet M, Guerra AJ, Puig T, Ciurana J. 3D-printed Tubular Scaffolds for Vascular Tissue Engineering. Procedia CIRP 2018; 68, 352-357.

[13] Rabionet M, Polonio E, Guerra A, Martin J, Puig T, Ciurana J. Design of a Scaffold Parameter Selection System with Additive Manufacturing for a Biomedical Cell Culture. Materials 2018; 11, 1427.

[14] Polonio-Alcalá E, Rabionet M, Guerra A, Yeste M, Ciurana J, Puig T. Screening of Additive Manufactured Scaffolds Designs for Triple Negative Breast Cancer 3D Cell Culture and Stem-Like Expansion. IJMS 2018; 19, 3148.

[15] Zhou K, Li Y, Zhang L, Jin L, Yuan F, Tan J, Yuan G, Pei J. Nano-micrometer surface roughness gradients reveal topographical influences on differentiating responses of vascular cells on biodegradable magnesium. Bioactive Materials 2021; 6, 262-272.

[16] Dong J, Pacella M, Liu Y, Zhao L. Surface engineering and the application of laser-based processes to stents - A review of the latest development. Bioactive Materials 2022; 10, 159-184.

[17] Katheng A, Kanazawa M, Iwaki M, Minakuchi S. Evaluation of dimensional accuracy and degree of polymerization of stereolithography photopolymer resin under different postpolymerization conditions: An in vitro study. The Journal of Prosthetic Dentistry 2021; 125, 695-702.